Nanoparticle Assemblies

DOI: 10.1002/ange.200501264

Nanoparticle Assemblies with Molecular Springs: A Nanoscale Thermometer**

*Jaebeom Lee, Alexander O. Govorov, and Nicholas A. Kotov**

Nanoparticle (NP) superstructures are important in the creation of smart materials with new functionalities. Most of the current examples of complex NP systems, such as bioconjugates[1–4] or hybrid nanocolloids[5] and their lattices,[6,7] are typically static: They show a limited response to environmental parameters and do not exhibit smooth reversible transitions of their three-dimensional organization or geometry in response to external stimuli. Dynamic NP superstructures with gradual structural adaptation to common physical parameters may reveal interesting analogies to biological entities of similar scale.[8,9] Additionally, such systems can find technological applications as optical devices. Herein we describe a reversible nanothermometer built from two types of NPs connected by a polymer acting as a molecular spring. The underlying microscopic mechanism of the nanothermometer involves plasmon resonance and exciton–plasmon interaction.

Poly(ethyleneglycol) (PEG) derivatives with *tert*-butoxycarbonyl (Boc) and *N*-hydroxysulfosuccinimide (NHS) groups at the terminal ends of the linear macromolecule (molecular weight 3400 Da, see *Experimental Section*) allow the sequential conjugation of one end to 20-nm Au NPs and of the other end to 3.7-nm CdTe NPs. This results in the superstructure depicted in the insert of Figure 1. The high-resolution transmittance electron microscopy (TEM) images of the product (Figure 2) confirm the formation of corona-like superstructures, although the density of the CdTe satellite particles distributed around the central gold core is lower than expected, probably owing to structural alterations during sample preparation. The CdTe colloid can be identified by the lattice plane spacing d of 0.352 ± 0.3 nm, which is typical for cubic CdTe.[10,11] The Au NPs show a d value of 0.23 ± 0.008 nm, which corresponds to the (111) planes of the Au crystal (see Supporting Information).

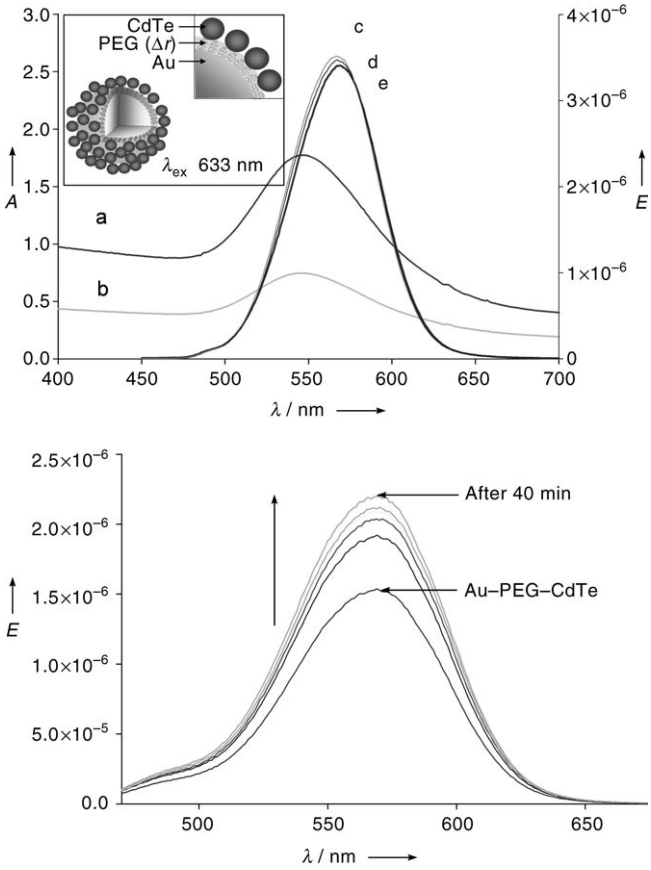

Figure 1. Top: Absorbance spectra of the PEG-conjugated Au NPs before (a) and after (b) removal of the Boc protecting groups; emission spectra of CdTe NPs after addition of EDC/NHS (c), after conjugation with Au–PEG (d), and of CdTe alone (e). Inset: Schematic drawing of the superstructure. Bottom: PL enhancement of the CdTe–PEG–Au superstructure after 40 min. A = absorbance, E = emission intensity.

The superstructure was excited with a He:Ne laser at 633 nm (20 mW, Uniphase, USA). The red light quanta result in efficient excitation of CdTe NPs, although these quanta are below the energy of the absorption threshold. This process is not as common as photoluminescence (PL) stimulated by light quanta with higher energy than the light emitted from

[*] Dr. J. Lee, Prof. Dr. N. A. Kotov
Department of Chemical Engineering
Department of Materials Science and Engineering and
Department of Biomedical Engineering
University of Michigan
Ann Arbor, MI 48109 (USA)
Fax: (+1) 734-764-7454
E-mail: kotov@umich.edu
Prof. Dr. A. O. Govorov
Department of Physics and Astronomy
Ohio University
Athens, OH 45701 (USA)

[**] This work was supported in part by an NSF-CAREER award (N.A.K.), NSF-Biophotonics (N.A.K.), AFOSR (N.A.K.), the University of Michigan (N.A.K.), and Ohio University (A.O.G.).

Supporting information for this article is available on the WWW under http://www.angewandte.org or from the author.

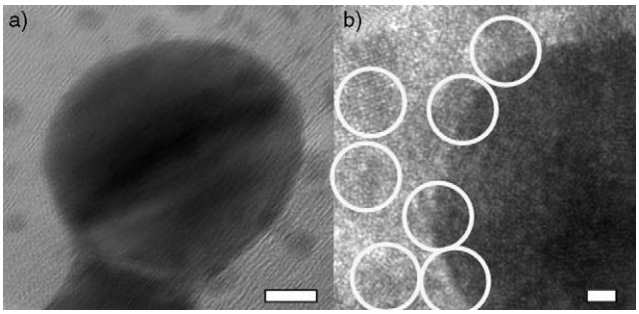

Figure 2. TEM images of the superstructure formed by conjugation of the CdTe NPs with the Au NPs: a) 5×10^5, and b) 10^6 magnification (in each case the bar represents 5 nm). The circles indicate the areas in which characteristic lattice fringes of 0.352 nm for the cubic zinc blende structure of CdTe can be seen after conjugation with PEG.

the NP, but it is well-documented for CdTe.[12,13] The mechanism of the excitation may include two-photon absorption as well as one-photon promotion of the charge carriers from thermally excited levels, yielding a complex curve with both second- and first-order dependence on the intensity of the incident light.[28] Regardless of the excitation pathway, luminescence induced by light below the absorption threshold is very useful for analytical applications because it allows effective elimination of the scattered light from the excitation source.

The similarity of the energies of the Au NP plasmon (549 nm) and the CdTe NP exciton (568 nm) results in resonance conditions in the superstructure (Figure 1). Once the exciton in the CdTe NP is generated, it induces oscillations of the electron density in the Au NP, that is, the plasmon. The resonance between them has two effects on the emission of CdTe: 1) It results in the enhancement of the luminescence intensity of the NPs at 568 nm, when the gap between the particles closes. In contrast to earlier reports on the fluorescence quenching of semiconductor colloids by gold particles,[14,15] we consistently observe a strong enhancement of the CdTe luminescence upon attachment of Au NPs, as long as certain geometrical rules are observed and the diameters selected match the resonance conditions.[16] The reasons behind this difference in observations can be understood from the theoretical description below. 2) The resonance conditions make the luminescence intensity very sensitive to the interparticle distance,[16] which is a convenient feature for analytical applications.[29,30] This complements the high signal-to-noise ratio that could result with two-photon emission. For a different geometrical arrangement—for instance, when a gold NP is attached to a CdTe nanowire, as described in our previous study[16]—a single Au NP may not produce any enhancement effect at all because of diffusion of the exciton along the nanowire. In this case, only the collective action of many NPs can provide a substantial enhancement of the emission.[16] Furthermore, the diameter of the Au NP also makes a substantial difference and, depending on the absorption peak of the Au colloid, one may not see any enhancement effect and even observe quenching of the semiconductor emission.

The temperature of the CdTe–PEG–Au dispersion was varied between 20 and 60 °C by a heating/cooling circulator (NESLAB, EX-111, USA). The conformation of the PEG can be altered as a response to the thermodynamic energy in the media. Despite the fact that PEG and PEO (poly(ethylene oxide)) have high critical temperatures, an increase in the temperature from 20 to 50 °C results in swelling of the PEG molecule and an increase in its diameter.[17,18] This alters the distance between the particles, which should produce a concomitant change in the luminescence output. Indeed, the superstructure shows a clear temperature dependence for the PL intensity. A high concentration of PEG segments attached to the Au surface can introduce additional differences compared to the classical case of diluted solutions of PEG.

A higher temperature leads to a decrease in the luminescence due to the more extended conformation of the PEG chain, and vice versa (Figure 3a, b). The non-PEG bonded system did not display any temperature dependence (see Supporting Information). Importantly, the process is totally reversible, showing less than 10% photodegradation with every temperature cycle (1500 s).

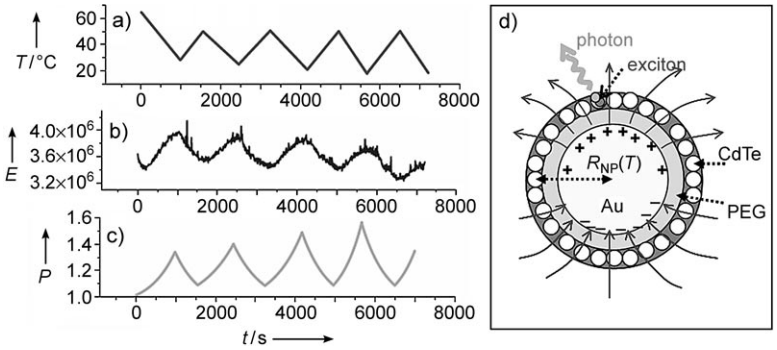

Figure 3. Variation in the PL intensity E (b) of the PEG-tethered Au and CdTe NPs depending on the temperature T (a); c) calculated photon-field enhancement factor P of the CdTe NPs as a function of time. d) Schematic representation of the dielectric model used for calculating the curve in (c) as well as the plasmon excitation with associated field lines; the plasmon excitation inside an Au nanosphere interacts with excitons in the CdTe NPs through electric fields. The distance $R_{NP}(T)$ varies with the temperature. The curve in (c) also represents a theoretical dielectric model of the NP assembly in which the CdTe NPs form a continuous spherical shell around the Au NP.

Calculations demonstrate that the change in the PEG-controlled distance between the NPs is the cause of the observed modulations in emission intensity. The photon-field enhancement factor P inside the CdTe NPs determines the probability of photon emission by an exciton trapped in a CdTe NP. Therefore, the emission intensity is proportional to the factor P [Eq. (1); where E_0 is the external electric field

$$P(\omega,R_{NP}) = \langle E^2\rangle_\Omega / E_0^2 \qquad (1)$$

inside a CdTe NP without the Au subsystem, E is the electric field in the presence of an Au NP averaged over the solid

angle Ω, R_{NP} is the position of the CdTe NPs with respect to the center of the superstructure (Figure 3d), and ω is the laser frequency].

We use here a simplified model which approximates a granular, molecular spring superstructure (Figures 1 and 2) as an Au sphere surrounded by polymer molecules and the CdTe shell (Figure 3d). We see no evidence of clustering of Au particles in the TEM images, which also supports the suggested theoretical model. Mathematical treatment of all CdTe NPs individually could be useful, but requires sophisticated numerical simulations. At the same time, a simple shell model reveals the physical essence of the phenomenon, which is important for the further development of similar superstructures. Note that the majority of Au NPs are faceted (see Supporting Information). While being mindful of the potential electric field aberrations caused by face edges, we consider them to be secondary effects in comparison to the model approximation.

Thus, treating an Au NP as a sphere and a collection of CdTe NPs as a spherical shell, we can analytically calculate the electric fields induced around the Au NP by matching the electrical boundary conditions and involving the first spherical harmonics.[19] After averaging over Ω, we obtain Equation (2), where B and C are complicated functions of the

$$P(\omega,R_{NP}) = \frac{|B| + 2|C^2|/R_{NP}^6}{E_0^2} \quad (2)$$

dielectric constants of the metal ($\varepsilon_m(\omega)$), PEG (ε_0), and CdTe ($\varepsilon_{CdTe} = 7.2$; see Supporting Information). In addition, the coefficients B and C are dependent on the radii of the spherical shells in our model. The function $\varepsilon_m(\omega)$ for the Au NPs was taken from reference [20]. Since the UV/Vis absorption of the Au NPs is dependent on the dielectric constant of the environment, the effective value of ε_0 of the surrounding media was taken as the dielectric constant of PEG (2.3).[21] Yun et al.[29] reported a $1/R^4$ dependence of fluorescence quenching by small Au NPs. The geometry of our system seems to be an even better match for $1/R^4$ distance dependence than that in reference [29], because the diameter of the Au NPs is large, and therefore the NP may behave like a surface. Nevertheless, Equation (2) (with $1/R^6$) was used because 1) a resonance process is better described by a dipole–dipole rather than a dipole–surface model, 2) it is a more general description, which could be applied for a variety of similar systems, and 3) expressions for corresponding coefficients are known, as opposed to those in the equation with $1/R^4$. R_{NP} was determined by the radius of gyration of PEG, R_{PEG}. On the basis of literature data,[22,23] R_{PEG} of PEG with a molecular weight of 3400 Da is 2–4 nm. The temperature-induced changes in the 20–60 °C range constitute 20–30 % of the polymer globule volume ratio, that is, changes in R_{PEG} of 0.6–1.2 nm.[24] In view of the fairly small change in the overall diameter of the Au–PEG–CdTe superstructure (ca. 26 ± 1.5 nm) caused by the conformational changes in PEG, the difference between the equations with $1/R^4$ and $1/R^6$ is not that essential here, except for the fact that a $1/R^6$ dependence should give stronger optical effects, which seems to be the case. Also note that light scattering plays a small role in the observed effect of luminescence enhancement. Assuming a linear dependence of $R_{PEG}(T) = 3\,\text{nm} + 1\,\text{nm}\,(T - 30\,°\text{C})/30\,°\text{C}$, one arrives at Equation (3). The high sensitivity of the NP

$$R_{NP}(T) = 11.8\,\text{nm} + R_{PEG}(T) = 14.8\,\text{nm} + (T - 30\,^o\text{C})/30\,^o\text{C} \quad (3)$$

emission to temperature in our superstructures arises from two factors: 1) The value of P rapidly decreases with Au–CdTe distance (approximately as R_{NP}^6), and 2) the exciton energy is very close to the plasmon resonance, which leads to a plasmon enhancement of emission. Equation (2) for the emission-enhancement factor has rather a complicated distance dependence caused by the multiple-shell structure. For $R_{NP} = 15$–16 nm, the plasmon-enhanced electric field and corresponding enhancement factor rapidly decrease with distance.

Compared with other approaches to sensing with nanocolloids,[4] the expansion and contraction of molecular springs represents a very sensitive transduction mechanism for chemical detection: Any change in the dimensions of the superstructure results in a shift of the plasmon resonance with respect to the exciton energy and subsequently in a reduction of the enhancement factor. Our theoretical analysis shows that, depending on the resonance conditions, the presence of Au can either increase or decrease the fluorescence of CdTe. For example, if the plasmon peak moves towards the exciton resonance with constriction of PEG, we may obtain the enhancement effect. If the plasmon peak is shifted away from the exciton energy, the fluorescence intensity can decrease. Substitution of $R_{NP}(T)$ into the equation for $P(\omega,R_{NP})$ for $\hbar\omega = 2.2$ eV, corresponding to a resonance wavelength of 568 nm, provides an analogue of the experimental $I(T)$ curve calculated in terms of photon-field enhancement factors (Figure 3c). The amplitude of the temperature zig-zag for $P(\omega,R_{NP})$ is about 30 %. This correlates very well with the variation of the emission intensity in our experiments (Figure 3a, b). The slightly lower amplitude registered in the experiment can be attributed to steric hindrance in the CdTe corona around the Au NP, preventing formation of the perfect CdTe NP shell assumed for our model. The linearity of the temperature response (Figure 3a) can be deceptive, because all the processes here are highly nonlinear. This becomes visible in the calculated results shown in Figure 3c.

Thus, the CdTe–PEG–Au system is an example of a nanoscale superstructure that undergoes a reversible structural change in response to the environmental conditions. The combination of this property with plasmon–exciton interactions that display a high sensitivity of the optical output on the distance modulations represents the foundation of a new family of sensing and optoelectronic devices.

Experimental Section

The CdTe NPs (3.7 nm in diameter with an emission at 568 nm) were synthesized according to the literature.[25] They were conjugated to the flexible spacer PEG and then linked to Au NPs (20 nm in diameter with a surface plasmon peak at 549 nm) to form molecular spring-type structures. The level of structural control necessary to produce molecular spring assemblies from NPs as shown in the insert

of Figure 1, rather than disorganized aggregates, was possible because the PEG oligomer had two different functional groups at the ends of the chain, NHS and Boc (Boc–NH–PEG–COO–NHS; molecular weight 3400 Da, Nektar, AL). The stabilizer, cetyltrimethylammonium bromide (CTAB, Aldrich, Milwaukee, WI) of the Au NPs was substituted with L-cysteine (Aldrich, Milwaukee, WI) in order to obtain the NH_2 functional group. The PEG (10 mg) was dissolved in deionized water (560 μL) and dimethyl sulfoxide (DMSO, 140 μL). This solution (700 μL) was mixed with the solution of the Au NPs (700 μL), and gently stirred at room temperature for 12 h. This procedure resulted in conjugation of the NHS terminus with NH_2 group of the NP stabilizer through a covalent amide linkage. Then the Boc protecting group was removed by treatment with trifluoroacetic acid (TFA, 5 μL) for 20 min.[26] The regenerated NH_2 terminus of PEG can be conjugated to a CdTe NP by standard conjugation techniques, that is, EDC/sulfo-NHS cross-linking,[16,27] resulting in covalent attachment of CdTe to the PEG chain on the end opposite to the Au NP.

Received: April 11, 2005
Revised: July 22, 2005
Published online: October 18, 2005

Keywords: excited states · luminescence · nanoparticles · poly(ethylene glycol) · thermal expansion

[1] M. Bruchez, Jr., M. Moronne, P. Gin, S. Weiss, A. P. Alivisatos, *Science* **1998**, *281*, 2013 – 2016.
[2] R. Levy, N. T. K. Thanh, R. C. Doty, I. Hussain, R. J. Nichols, D. J. Schiffrin, M. Brust, D. G. Fernig, *J. Am. Chem. Soc.* **2004**, *126*, 10076 – 10084.
[3] C. A. Mirkin, R. L. Letsinger, R. C. Mucic, J. J. Storhoff, *Nature* **1996**, *382*, 607 – 609.
[4] C. M. Niemeyer, *Biochem. Soc. Trans.* **2004**, *32*, 51 – 53.
[5] T. Mokari, E. Rothenberg, I. Popov, R. Costi, U. Banin, *Science* **2004**, *304*, 1787 – 1790.
[6] D. V. Talapin, E. V. Shevchenko, C. B. Murray, A. Kornowski, S. Foerster, H. Weller, *J. Am. Chem. Soc.* **2004**, *126*, 12984 – 12988.
[7] A. L. Rogach, *Angew. Chem.* **2004**, *116*, 150 – 151; *Angew. Chem. Int. Ed.* **2004**, *43*, 148 – 149.
[8] F. R. Aussenegg, H. Brunner, A. Leitner, C. Lobmaier, T. Schalkhammer, F. Pittner, *Sens. Actuators B* **1995**, *29*, 204 – 209.
[9] T. Schalkhammer, C. Lobmaier, F. Pittner, A. Leitner, H. Brunner, F. R. Aussenegg, *Sens. Actuators B* **1995**, *24*, 166 – 172.
[10] N. Gaponik, D. V. Talapin, A. L. Rogach, K. Hoppe, E. V. Shevchenko, A. Kornowski, A. Eychmueller, H. Weller, *J. Phys. Chem. B* **2002**, *106*, 7177 – 7185.
[11] Z. Tang, N. A. Kotov, M. Giersig, *Science* **2002**, *297*, 237 – 240.
[12] M. Goppert-Mayer, *Ann. Phys.* **1931**, *9*, 273 – 294.
[13] A. G. Joly, W. Chen, D. E. McCready, J. O. Malm, J. O. Bovin, *Phys. Rev. B* **2005**, *71*, 165304.
[14] S. Chen, K. Kimura, *Chem. Lett.* **1999**, 233 – 234.
[15] Z. Gueroui, A. Libchaber, *Phys. Rev. Lett.* **2004**, *93*, 166108.
[16] J. Lee, A. O. Govorov, J. Dulka, N. A. Kotov, *Nano Lett.* **2004**, *4*, 2323 – 2330.
[17] C. Branca, A. Faraone, S. Magazu, G. Maisano, P. Migliardo, V. Villari, *J. Mol. Struct.* **1999**, *482–483*, 503 – 507.
[18] C. Branca, S. Magazu, G. Maisano, P. Migliardo, V. Villari, *J. Phys. Condens. Matter* **1998**, *10*, 10141 – 10157.
[19] L. D. Landau, E. M. Lifshitz, *Electrodynamics of Continuous Media*, Pergamon, New York, **1960**, p. 413.
[20] M. Quinten, *Z. Phys. B* **1996**, *101*, 211 – 217.
[21] U. Raviv, J. Frey, R. Sak, P. Laurat, R. Tadmor, J. Klein, *Langmuir* **2002**, *18*, 7482 – 7495.
[22] J. D. Ferry, *Viscoelastic Properties of Polymers*, 3rd ed., Wiley, New York, **1980**.
[23] A. F. M. Barton, *CRC Handbook of Polymer–Liquid Interaction Parameters*, CRC, Boca Raton, FL, **1990**.
[24] J. C. Munro, C. W. Frank, *Langmuir* **2004**, *20*, 3339 – 3349.
[25] A. L. Rogach, D. V. Talapin, H. Weller in *Colloids and Colloidal Assembly* (Ed.: F. Caruso), Wiley-VCH, Weinheim, **2004**, pp. 52 – 95.
[26] S. Westenhoff, N. A. Kotov, *J. Am. Chem. Soc.* **2002**, *124*, 2448 – 2449.
[27] G. T. Hermanson, *Bioconjugate Techniques*, Academic Press, San Diego, **1995**, p. 786.
[28] B. Ozturk, J. Lee, N. A. Kotov, unpublished results.
[29] C. S. Yun, A. Javier, T. Jennings, M. Fisher, S. Hira, S. Peterson, B. Hopkins, N. O. Reich, G. F. Strouse, *J. Am. Chem. Soc.* **2005**, *127*, 3115 – 3119.
[30] C. Sönnichsen, B. M. Reinhard, J. Liphardt, A. P. Alivisatos, *Nature Biotechnol.* **2005**, *23*,741 – 745.

